

Research Article

Micromechanical Thermal Assays of Ca^{2+} -Regulated Thin-Filament Function and Modulation by Hypertrophic Cardiomyopathy Mutants of Human Cardiac Troponin

Nicolas M. Brunet,^{1,2,3} Goran Mihajlović,^{4,5} Khaled Aledealat,^{4,6} Fang Wang,^{1,7} Peng Xiong,^{4,8} Stephan von Molnár,^{4,8} and P. Bryant Chase^{1,8}

¹ Department of Biological Science, The Florida State University, P.O. Box 3064295, Tallahassee, FL 32306, USA

² Institute of Molecular Biophysics, The Florida State University, Tallahassee, FL 32306, USA

³ Donders Institute for Brain, Cognition and Behavior, Centre for Cognitive Neuroimaging, Radboud University Nijmegen, 6500 HB Nijmegen, The Netherlands

⁴ Department of Physics, The Florida State University, Tallahassee, FL 32306, USA

⁵ San Jose Research Center, Hitachi Global Storage Technologies, San Jose, CA 95135, USA

⁶ Department of Physics, Jordan University of Science and Technology, Irbid 22110, Jordan

⁷ Department of Neurobiology, College of Basic Medical Science, Southern Medical University, Guangzhou 510515, China

⁸ Integrative NanoScience Institute (INSI), The Florida State University, Tallahassee, FL 32306, USA

Correspondence should be addressed to P. Bryant Chase, chase@bio.fsu.edu

Received 2 August 2011; Accepted 2 November 2011

Academic Editor: Seunghun Hong

Copyright © 2012 Nicolas M. Brunet et al. This is an open access article distributed under the Creative Commons Attribution License, which permits unrestricted use, distribution, and reproduction in any medium, provided the original work is properly cited.

Microfabricated thermoelectric controllers can be employed to investigate mechanisms underlying myosin-driven sliding of Ca^{2+} -regulated actin and disease-associated mutations in myofilament proteins. Specifically, we examined actin filament sliding—with or without human cardiac troponin (Tn) and α -tropomyosin (Tm)—propelled by rabbit skeletal heavy meromyosin, when temperature was varied continuously over a wide range (~ 20 – 63°C). At the upper end of this temperature range, reversible dysregulation of thin filaments occurred at pCa 9 and 5; actomyosin function was unaffected. Tn-Tm enhanced sliding speed at pCa 5 and increased a transition temperature (T_i) between a high activation energy (E_a) but low temperature regime and a low E_a but high temperature regime. This was modulated by factors that alter cross-bridge number and kinetics. Three familial hypertrophic cardiomyopathy (FHC) mutations, cTnI R145G, cTnI K206Q, and cTnT R278C, cause dysregulation at temperatures ~ 5 – 8°C lower; the latter two increased speed at pCa 5 at all temperatures.

1. Introduction

Biomolecular motors have clear promise for transport applications in micro- and nanofabricated devices although control of motion remains a major challenge [1–4]. Toward that end, we constructed a microfabricated thermoelectric controller for rapid and reversible actuation using myosin, the biomolecular motor of muscle, and its partner filament, actin [5, 6]. Thermal control of kinesin-microtubule motility using thermally responsive polymers has also been demonstrated as a possible temperature-dependent control mechanism for biomolecular motors [7]. We present here novel applications of our thermoelectric control system to

investigate changes in actin-myosin motility when Ca^{2+} -regulated thin (actin) filaments are used, and when thin-filament Ca^{2+} -regulatory protein mutations are introduced that underlie an inherited cardiovascular disease, familial hypertrophic cardiomyopathy (FHC) [8–10]. Results provide insights into mechanisms of altered function when thin filaments are reconstituted with human cardiac Ca^{2+} -regulatory proteins troponin (Tn) and tropomyosin (Tm), and further modulated by FHC-related mutations in cardiac Tn.

In the heart—and in vertebrate striated muscles in general—contraction is physiologically controlled by binding of cytoplasmic Ca^{2+} to thin filaments. Thin filaments are comprised of three major proteins: actin, Tm, and Tn that

is itself a complex of three polypeptides [11]. Ca^{2+} activates thin filaments by binding to Tn, leading to structural changes that ultimately expose myosin-binding sites on actin subunits [11]. Our previous work on the thermoelectric controller utilized only myosin and unregulated F-actin, that is, Ca^{2+} -independent motility achieved using actin filaments without Tn or Tm [5, 6]. This study was initiated because Ca^{2+} -regulated thin filaments could have several advantages over unregulated F-actin in a thermoelectric nanoactuator. First, Ca^{2+} would provide a secondary control mechanism that is separate from temperature. An additional benefit is that the Ca^{2+} -regulatory proteins Tn and Tm at saturating Ca^{2+} can enhance function of the actomyosin system [12–20]. These effects of Tn and Tm on actomyosin function, however, appear to vary markedly over the limited temperature ranges studied previously [16, 18, 21] and thus could introduce nonlinearities to a thermoelectric nano-actuator.

Temperature has obvious physiological relevance as a determinant of mammalian striated muscle contraction. It affects several fundamental aspects of muscle structure and function [22–24] although temperature effects on muscle function appear to be greater at low temperatures used in many experiments than at physiological temperature; examples are isometric tetanic tension [25–27] and maximum mechanical power output [28]. Temperature also modulates the control of striated muscle contraction by Ca^{2+} regulatory proteins Tn and Tm, although there are both qualitative and quantitative discrepancies on this point in the striated muscle literature [22, 26, 29, 30]. Interestingly, mild hypothermia has been reported to be a positive inotropic effector in living cardiac muscle due to interplay between temperature and cardiac thin filament Ca^{2+} regulation [31]. Our thermoelectric controller allows us to address these issues and more in a single experiment through rapid exploration of broad temperature regimes surrounding physiological temperature.

Some mutations in Tn and Tm alter thin-filament function in ways that might make the mutant proteins useful in biomolecular motor-based transport applications. In particular, mutations associated with familial hypertrophic cardiomyopathy (FHC)—one of a growing number of diseases caused by mutations in the genes for sarcomere proteins including thin-filament Ca^{2+} -regulatory proteins [8–10]—may be especially useful in bionanomechanical systems even though those mutations are devastating for patients [32–41]. The molecular basis by which these mutations alter thin-filament function and bring about cardiovascular disease is unknown [8, 10, 42]. Our thermoelectric controller could provide important insight into mechanisms by which these mutations in myofibrillar proteins alter contractile function, and directly or indirectly signal changes in gene expression that underlie the progression to pathological cardiac hypertrophy in FHC.

2. Materials and Methods

2.1. Protein Preparations: Myosin, Heavy Meromyosin, Actin, Troponin, and Tropomyosin. Florida State University's Institutional Animal Care and Use Committee approved all

procedures and protocols involving vertebrate animals. Adult New Zealand White rabbits were housed in Florida State University's Laboratory Animal Resources facility and were handled in accordance with the current National Institutes of Health/National Research Council Guide for the Care and Use of Laboratory Animals. Briefly, rabbits were injected IM with 3 mg Acepromazine + 10 mg/kg Xylazine + 50 mg/kg Ketamine. Following verification of appropriate surgical depth of anesthesia, the rabbits were exsanguinated via laceration of the carotid artery. The euthanized animals were skinned, eviscerated, and chilled on ice. Back and leg muscles were removed for acetone powder, or back muscles only for myosin preparation [12, 13, 43]. Myosin and the soluble chymotryptic digest fragment heavy meromyosin (HMM) were prepared from fast skeletal muscle as described [12, 13, 43, 44]. HMM was made from myosin stored <5 weeks in glycerol (1 : 1) at -20°C ; HMM was used within 3 days after preparation. Rabbit muscle actin was purified from muscle acetone powder as described [12, 13, 43, 45]. F-actin was labeled with rhodamine phalloidin (RhPh; Molecular Probes) for fluorescence microscopy (Figure 1(a)). F-actin ($33\ \mu\text{g}/\text{mL}$) and RhPh ($1\ \mu\text{M}$) were incubated in actin buffer (AB) with 1 mM DTT at 4°C overnight; fluorescently labeled F-actin was stable at 4°C for at least 2 weeks.

Recombinant human α -Tm was expressed in *E. coli* as a homodimeric fusion protein with maltose binding protein (MBP); α -Tm was purified following removal of the MBP affinity tag via thrombin cleavage [13, 33]. After removal of the MBP tag, recombinant α -Tm has two extra amino acids (GS-) at the N-terminus; GS- is a conservative alternative to the AS-dipeptide in bacterially expressed Tm that substitutes functionally for acetylation of Tm's N-terminus [46, 47]. Purified Tn from human cardiac muscle (cTn) was obtained from Research Diagnostics (Flanders, NJ), or coexpressed recombinantly (rHcTn) in *E. coli* as a fusion protein with glutathione S-transferase (GST); the ternary rHcTn complex was purified following removal of the GST affinity tag via cleavage with TEV protease [13]. FHC mutations of rHcTn were introduced via site-directed mutagenesis to the bacterial coexpression plasmid; changes were verified by DNA sequencing. Proteins were assessed by coomassie-stained Tricine-SDS PAGE [48] and quantitative analysis with a Kodak EDAS 290 digital imaging system.

2.2. In Vitro Motility Assays. The speed of RhPh F-actin over HMM-coated surfaces was measured to assess the kinetics of actomyosin interactions and, for reconstituted thin filaments, their regulation by Ca^{2+} . All aspects of the motility experiments with unregulated F-actin, such as flow cell assembly, solution preparation, assay procedures, and data collection were conducted as described [5, 13, 43, 49]. [HMM] applied to flow cells was $250\ \mu\text{g}\ \text{mL}^{-1}$ in the majority of assays to achieve high density of HMM (ρ) on the nitrocellulose-coated motility surface; to reduce ρ in a limited set of experiments, $75\ \mu\text{g}\ \text{mL}^{-1}$ HMM was applied to the flow cell.

The standard motility buffer (MB) contained 10 mM ethylene glycol-bis(2-aminoethylether)-N,N,N',N'-tetraacetic

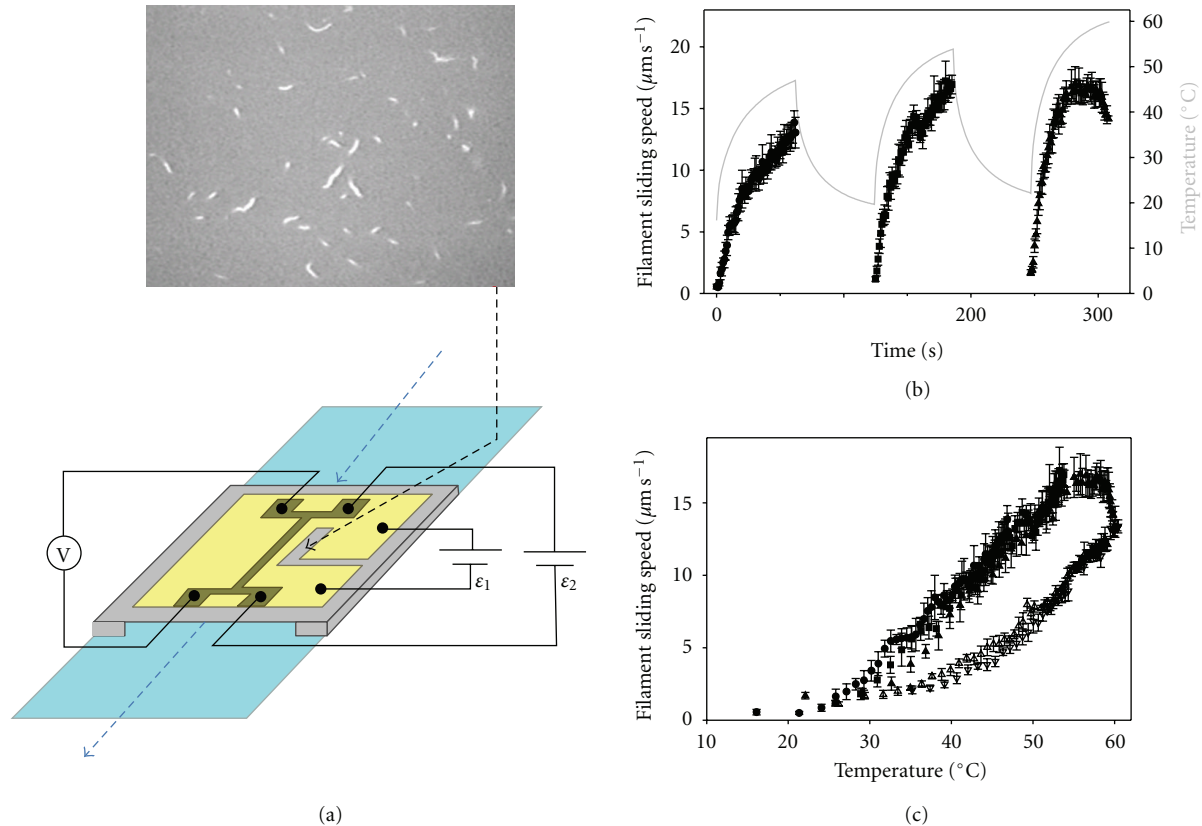


FIGURE 1: Temperature dependence of HMM-driven sliding of RhPh-labeled actin filaments determined using a microfabricated thermoelectric heater. (a) Modified flow cells were constructed as described [5]. Flow cells consisted of a microscope slide (light blue) and a modified cover slip (gray and gold), separated by two, thin spacers and held together by nonfluorescent vacuum grease. Solutions (Section 2.2) are pipetted through the flow cell as indicated by the blue, dashed arrows. To warm the flow cell, current is injected via circuit ϵ_1 into a microfabricated thermoelectric heater (gold) on the coverslip's outer surface; flow cells are cooled by circulating chilled water through a copper coil wrapped around the microscope objective. Temperature is monitored via a linear, resistive thermometer (dark gold structure) that was microfabricated on the inner face of the coverslip (i.e., on the same side where actomyosin motility occurred, and opposite to the side with the thermoelectric heater); temperature is obtained from a calibrated voltage readout (V) with bias current set by circuit ϵ_2 . Motion of fluorescently labeled filaments on the inner side of the coverslip (top micrograph) is observed and recorded through a window (black, dashed arrow) located immediately adjacent to the thermometer. (b) Time course of temperature (gray line; right ordinate) and sliding speed (solid symbols; left ordinate) for regulated thin filaments (F-actin plus native cTn and α -Tm) at pCa 5 during the heating phase of three cycles of heating and cooling (Section 2). Points represent mean \pm S.D. of the sliding speed for 3–8 filaments during 1 s. Note that the upper limit of the temperature-dependent increase in sliding speed occurs at $\sim 54^\circ\text{C}$ ($t > 4.5$ min). (c) The data from (b) were replotted to eliminate time: cycle 1 (●), cycle 2 (■), and cycle 3 (▲). An additional dataset for unregulated F-actin sliding is shown: cycle 1 (△) and cycle 2 (∇). Note that the sliding speed of regulated thin filaments at the highest temperature is almost the same as for unregulated F-actin.

acid (EGTA), 20 mM 3-(N-Morpholino)propanesulfonic acid (MOPS), $[\text{K}^+] = 50$ mM, $[\text{Na}^+] = 15$ mM, pMg 3 (pMg = $-\log_{10}[\text{Mg}^{2+}]$, where $[\text{Mg}^{2+}]$ is in molar units), and appropriate amounts of Tris⁺, and acetate (anion) to obtain an ionic strength of 0.085 M at pH 7. Concentrations of Ca^{2+} , Mg^{2+} , Na^+ , K^+ were determined taking into account known metal ion binding constants and their enthalpies [32, 50]; solution composition was chosen to minimize enthalpic changes in pH in flow cells when temperature was varied. Glucose (3 mg/mL), 0.1 mg/mL glucose oxidase, 0.018 mg/mL catalase (Boehringer-Mannheim), and 40 mM dithiothreitol (DTT) were added immediately prior to an assay to minimize photooxidation and photobleaching [49]. Experiments were conducted at saturating $[\text{Ca}^{2+}]$ (pCa 5, where pCa = $-\log_{10}[\text{Ca}^{2+}]$, with $[\text{Ca}^{2+}]$ in molar units) or,

where indicated, at low $[\text{Ca}^{2+}]$ (pCa 9); note that $[\text{Ca}^{2+}]$ does not affect sliding speed of unregulated F-actin [12, 14]. Methylcellulose (final concentration 0.3%), dialyzed against sodium azide (0.02%), was added to MB to prevent actin filament diffusion away from the assay surface [12, 49, 51]. Solutions for assays with reconstituted thin filaments were the same as for unregulated F-actin, except for the last two solutions: the buffer applied to the flow cell before MB contained 75 nM each of α -Tm and either native cTn or recombinant hcTn and was incubated for three minutes before infusing MB containing the same concentrations of Tn and Tm [12, 13, 32, 50]. The minimum concentrations of native or WT Tn and Tm added to MB to obtain well-regulated filaments at 30°C were determined by titrations and applying the following criteria: filament sliding was

TABLE 1: Metabolite concentrations in standard and modified motility buffers.

Metabolites	Standard ¹	Modified solutions for motility assays ²		
	Motility buffer	Control	High Pi	Low ATP
[ATP]	2 mM	2 mM	2 mM	0.2 mM
Sucrose phosphorylase	—	5.3 $\mu\text{g}/\text{mL}$	—	5.3 $\mu\text{g}/\text{mL}$
Sucrose	—	10 mM	10 mM	10 mM
[Pi]	$\sim 10 \mu\text{M}$	$\sim 1 \mu\text{M}$	4 mM	$\sim 1 \mu\text{M}$
Creatine kinase (CK)	—	0.1 mg/mL	0.1 mg/mL	0.1 mg/mL
Creatine (Cr)	—	30 μM	30 μM	12 μM
Creatine phosphate (CP)	—	1 mM	1 mM	1 mM
[ADP]	$\sim 10 \mu\text{M}$	0.42–0.57 μM	0.42–0.57 μM	$\sim 0.02 \mu\text{M}$

Values for [ATP], [Pi], and [ADP] represent final concentrations in motility buffers. [Pi] in columns 3 and 5 were estimated using $K_{\text{eq}} = 0.06$ for the reaction $\text{sucrose} + \text{Pi} \rightarrow \alpha\text{-D-glucose-1-phosphate} + \text{D-fructose}$ [52, 54]. [ADP] estimates are based on the equilibrium constant (K_{eq}) for the reaction $\text{ATP} + \text{Cr} \rightarrow \text{ADP} + \text{CP}$, and are given in columns 3–4 with lowest and highest value corresponding to the lowest (27°C) and highest (42°C) temperatures employed, respectively. The estimate of [ADP] in column 2 was based on Chase and Kushmerick [53].

¹Motility buffer (MB) employed in the majority of experiments (data in Figures 1–4) did not include sucrose phosphorylase and creatine kinase.

²Modified motility buffers were used for experiments shown in Figure 5.

inhibited at pCa 9, while motility was fast and uniform at pCa 5 and standard temperature of 30°C [12, 13, 32, 50]. In a limited set of motility experiments, standard MB was modified to vary metabolite concentrations (Table 1) as follows: either 5.3 $\mu\text{g}/\text{mL}^{-1}$ sucrose phosphorylase and 10 mM sucrose were added to reduce inorganic phosphate (Pi) [52] or acetate was partially replaced by Pi to achieve the high Pi condition (sucrose phosphorylase was not added); contaminating ADP was reduced to $<1 \mu\text{M}$ by addition of creatine phosphate (CP) and creatine phosphokinase (CK) [53].

Motility data were collected while varying temperature by employing modified flow cells containing microfabricated Au heater and thermometer elements (Figure 1(a)), where the thermometer is located immediately adjacent to the viewing region [5]. In experiments using the thermoelectric heater, cooling was achieved by circulating chilled water through a copper coil wrapped around the microscope objective; in a limited set of experiments, assays at constant temperature were achieved by circulating temperature-controlled water through the coil surrounding the objective [13, 43]. Motility speed was analyzed using MetaMorph software (Universal Imaging) as described [5]. Stacks of frames (one stack for each second of temperature transient data, or 10–12 stacks for each constant temperature experiment from one flow cell) were created from digitized movies.

2.3. Statistical Analyses. Averages and error estimates were calculated with Microsoft Excel 2000. Averages are given as unweighted mean \pm SD. Linear regression analyses were performed using Microsoft Excel 2000 or SigmaPlot (Windows versions 8.0 and 11.2; SPSS Inc., Chicago, IL); nonlinear regression analyses were performed using SigmaPlot.

A transition temperature (T_t) was estimated from Arrhenius transformed speed versus temperature data that exhibited a change in slope with temperature. To obtain T_t , the data were divided into two parts (high- and low-temperature regimes) that were separated by two adjacent points on the Arrhenius plot's temperature axis; several such

divisions of each dataset were processed using the following algorithm. Linear regressions were obtained for each regime, and the intersection point determined for those regressions. In general, the intersection point does not fall between the two data points that separate the high and low temperature regimes. The small number of intersection points that did fall between the high- and low-temperature regimes were considered to be candidates for T_t ; in the few instances when there was more than one candidate point, the median value was chosen for T_t .

3. Results

3.1. Temperature Dependence of Unregulated F-Actin and Regulated Thin-Filament Sliding. To examine sliding of Ca^{2+} -regulated thin filaments over a broad range of temperatures, we employed a thermoelectric controller (Figure 1(a)) that enables both rapid and continuous variation of a flow cell's temperature [5]. Figure 1(b) shows sliding speed (solid symbols) as a function of time for thin filaments reconstituted with native cTn· α -Tm at pCa 5 during three heating phases of cyclic heating and cooling (~ 20 – 60°C). Note that the peak temperature (gray line) increased with each cycle. Speed increased with temperature during the heating phase of each cycle over most of the range examined. As temperature increased during the third cycle, however, sliding speed of regulated actin reached a maximum at $\sim 54^\circ\text{C}$, and then speed declined above $\sim 58^\circ\text{C}$ (Figure 1(b)). This anomalous decline in speed for regulated thin filaments is particularly evident in Figure 1(c), solid symbols where data from all three heating cycles of Figure 1(b) were combined to show the temperature dependence of sliding speed. Superposition of the data from three cycles suggests that brief exposure to elevated temperature over at least the first two cycles was fully reversible.

Comparison of regulated versus unregulated F-actin sliding speed at high temperature suggests that the anomalous decline for regulated thin-filament speed is more likely due to an effect of temperature on Tn·Tm rather than on

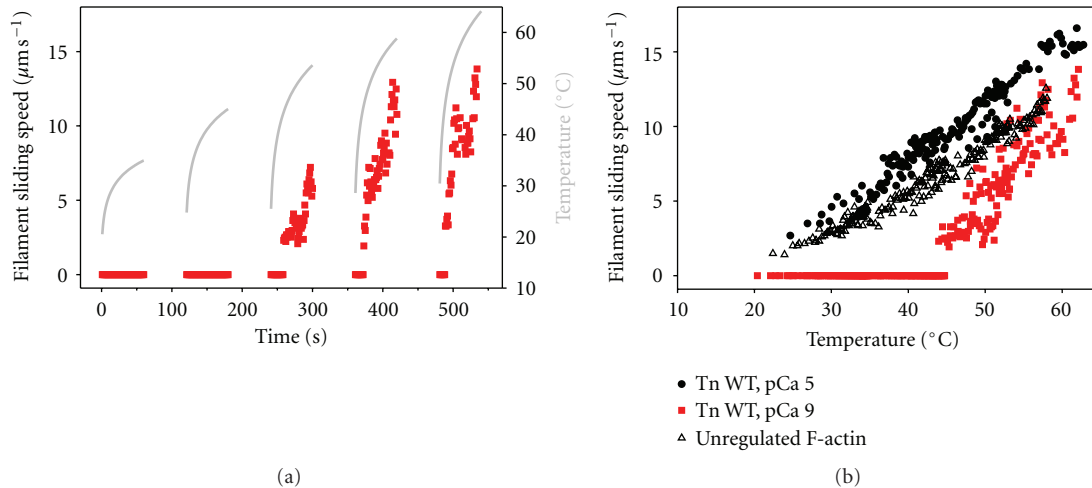


FIGURE 2: Thin filaments remain motile but lose Ca^{2+} -regulation at high temperature. (a) Time course of temperature (gray line; right ordinate) and sliding speed (solid squares, red fill; left ordinate) for regulated thin filaments (F-actin plus rhcTn and α -Tm) at pCa 9 during the heating phase of five cycles of heating and cooling. Points represent the mean sliding speed for 3–5 filaments during 1 s. At pCa 9, nonzero sliding speeds in heating cycles 3–5 indicate loss of Ca^{2+} -regulation (dysregulation); note that temperature-dependent loss of Ca^{2+} -regulation is fully reversible following cooling (beginning of cycles 4–5). (b) Data from (a) (pCa 9; solid squares, red fill) were replotted to eliminate time. Additional data for regulated thin filaments (F-actin plus rhcTn and α -Tm) at pCa 5 (●) and unregulated F-actin (Δ) from the same series of experiments are also shown for comparison.

actin or HMM. Regulated filament speed at pCa 5 (solid symbols) was at least as fast as that for unregulated F-actin (open symbols) at each temperature over the range examined (~ 20 – 60°C) (Figure 1(c)), consistent with previous reports over more limited temperature ranges [12, 13, 16, 20]. The speed of unregulated F-actin, however, increased continuously over the entire temperature range—even at the highest temperatures examined, where regulated thin-filament speed declined. To test the hypothesis that Tn·Tm is responsible for the anomalous decline in speed (Figure 1), we examined the effect of temperature on regulated thin-filament motility at pCa 9, that is, in the absence of activating Ca^{2+} . Figure 2(a) shows sliding speed (red symbols) as a function of time for thin filaments reconstituted with rHcTn· α -Tm at pCa 9 during five heating phases of cyclic heating and cooling. Note that the peak temperature (gray line) increased with each cycle, as in Figure 1(b). Data from all five heating cycles of Figure 2(a) were combined to show the temperature dependence of sliding speed in Figure 2(b). As expected in the absence of Ca^{2+} , regulated thin filaments exhibited little or no motion (note red symbols at speed ~ 0) over a broad range of temperatures (~ 20 – 43°C). Above $\sim 43^\circ\text{C}$, filament sliding was observed indicating loss of Ca^{2+} regulation (red symbols; Figure 2) although the average speed was generally less than or similar to that of unregulated F-actin (open symbols; Figure 2(b)). As for native cTn (Figure 1(c), solid symbols), rHcTn WT regulated thin filaments at pCa 5 (Figure 2(b), solid symbols) were faster than unregulated F-actin (Figure 2(b), open symbols); an anomalous decline in speed with WT rHcTn (Figure 2(b), solid black circles) occurred at slightly a higher temperature (by ~ 4 – 5°C) than for native cTn (Figure 1(c), solid symbols), suggesting increased stability of the recombinantly expressed protein or its interactions with

F-actin- α -Tm. The apparent loss of Ca^{2+} -regulation, indicated in Figure 2 by thin filament sliding (nonzero speeds) at pCa 9 for temperatures above $\sim 43^\circ\text{C}$, is completely reversible because thin-filaments stopped moving after temperature was lowered during the cooling phase of each cycle at pCa 9 (Figure 2(a)).

Arrhenius analysis of the data in Figure 1(c) reveals that the activation energy (E_a) for regulated thin-filament speed at pCa 5 exhibited two distinct values, with a change in the slope at $T_t \sim 38^\circ\text{C}$ (Figure 3, solid symbols and black solid lines). For regulated thin filaments (Figure 3, solid symbols and black solid lines), E_a at temperatures below physiological (100.4 kJ/mol) was >2 -fold greater than E_a for the higher-temperature regime (41.8 kJ/mol), while the latter value was closer to that of unregulated F-actin (61.9 kJ/mol) (Figure 3, open symbols and black dashed line). Temperature has a dramatic, nonlinear effect on the viscosity of water [55], and the speed of filament sliding varies inversely with solvent viscosity [43, 56]; we therefore asked whether temperature-dependent changes in solvent viscosity could explain the nonlinear Arrhenius relation (Figure 3). The data in Figure 3 were processed to remove the temperature dependence of solvent viscosity by first normalizing viscosity with respect to that of water at 37°C (i.e., body temperature), and second assuming that speed varies inversely with solvent viscosity [43, 56]. After removing the effects of viscosity, slopes of the Arrhenius plots were reduced (Figure 3, blue lines). E_a for unregulated F-actin decreased from 61.9 kJ mol^{-1} to 47.0 kJ mol^{-1} (Figure 3, blue dashed line). For regulated thin filaments, E_a decreased from 100.4 to 83.9 kJ mol^{-1} for $T < 38^\circ\text{C}$, and from 41.8 to 26.6 kJ mol^{-1} for $T > 38^\circ\text{C}$ (Figure 3, black versus blue solid lines). The latter value of E_a is suggestive of a diffusion-limited process, in accord with the previously observed inverse relationship between

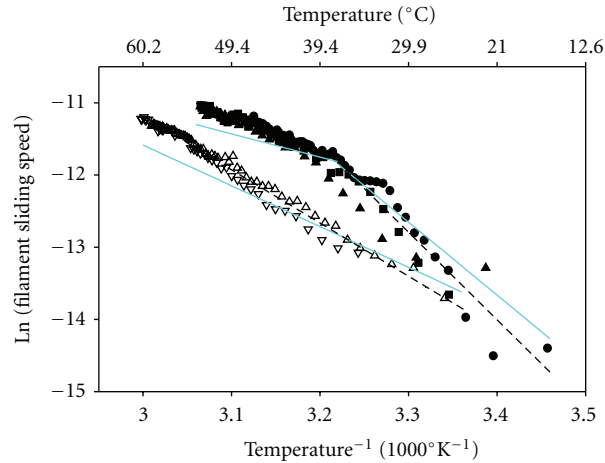


FIGURE 3: Correction for temperature-dependent effects of solvent viscosity (solid, cyan lines) on filament sliding speed of regulated thin filaments (solid symbols) and unregulated F-actin (open symbols). Data from Figure 1(c) were replotted in Arrhenius form (symbols as in Figure 1), with data omitted for regulated thin filaments above $\sim 54^\circ\text{C}$ and filament sliding speeds expressed in $\mu\text{m s}^{-1}$. Dashed lines (black) are linear least squares regressions on the data before correction for temperature-dependent changes in solvent viscosity. Note the change in slope at $\sim 38^\circ\text{C}$ (T_t) for regulated thin filaments. Effects of temperature-dependent changes in solvent viscosity (normalized to that at body temperature, 37°C) were removed by assuming that speed varies inversely with viscosity, as demonstrated experimentally [43]; the net result of this correction in all instances is a decrease in apparent E_a .

speed and viscosity [43, 56]. Despite the reduction of slopes for regulated thin-filaments, the ratio of E_a 's between the two temperature regimes increased from 2.4 to 3.1. Below 38°C , the ratio of E_a 's for regulated thin-filament sliding speed with respect to that of unregulated F-actin increased from 1.6 to 1.8. It is clear from this analysis that it is important to consider temperature-dependent changes in solvent viscosity when evaluating actin filament sliding speed. Nonlinearities in the Arrhenius plot (Figure 3), however, cannot be explained by temperature-dependent changes in solvent viscosity.

3.2. Influence of FHC Mutations in Troponin on the Temperature Dependence of Thin-Filament Sliding. Because the temperature dependence of maximum filament sliding speed is influenced by the presence and function of $\text{Tn}\cdot\text{Tm}$ (Figures 1–3), and FHC-related mutations in troponin profoundly influence the Ca^{2+} dependence of myofilament function [8–10, 57], we utilized the thermoelectric controller to investigate temperature effects on thin filaments reconstituted with $\text{rHcTn}\cdot\alpha\text{-Tm}$ when one of three FHC-related mutations— TnI R145G , TnI K206Q , or TnT R278C —was incorporated into the troponin complex (Section 2). At $\text{pCa } 5$, filament sliding speed for two mutants (TnI K206Q and TnT R278C) was faster than WT over the range of temperatures examined, consistent with previously reported data for TnI K206Q using recombinant rat cardiac Tn [32]. In contrast, speed with TnI R145G was similar to WT (Figure 4).

The micromechanical thermal assays with thin filaments containing FHC mutations in rHcTn suggest that either the mutant troponins are intrinsically less thermally stable, or the regulatory interaction of mutant troponin with F-actin- $\alpha\text{-Tm}$ is less stable, or both (Figure 4(a)). All three of the FHC mutants exhibited anomalous declines in speed

at lower temperatures than WT rHcTn , with the cTnT R278C and cTnI R145G mutations resulting in $\sim 4\text{--}5^\circ\text{C}$ decreases, and the cTnI K206Q mutation leading to a larger, $\sim 8\text{--}9^\circ\text{C}$ decrease in the temperature at which the anomalous decline in speed occurred as temperature continued to rise (Figure 4(a)).

Arrhenius analysis suggests that there was little effect of the FHC mutations on T_t for thin filaments reconstituted with WT or mutant rHcTn , with values of $38\text{--}41^\circ\text{C}$ where they could be unambiguously determined (Figure 4(b)). This was similar to the value of $T_t = \sim 38^\circ\text{C}$ obtained with native cTn (Figure 3). The slopes of the high- and low-temperature regimes were more similar for the two fastest mutants (cTnT R278C and cTnI K206Q) compared with WT or the cTnI R145G mutant (Figure 4(b)); in fact, it was not possible to unambiguously identify a value of T_t from data with TnI K206Q by the algorithm used (Section 2). When the data for unregulated F-actin from Figure 2(b) (open symbols) were plotted in Arrhenius form (Figure 4(b), gray dashed lines), a value of $T_t \sim 33^\circ\text{C}$ was obtained in contrast to the dataset in Figures 1 and 3, where T_t for unregulated F-actin could not be determined because there were not sufficient points below T_t to define a low-temperature regime.

3.3. Influence of Factors that Affect Cross-Bridge Number and Kinetics on Temperature Dependence of Unregulated F-Actin and Regulated Thin-Filament Sliding Speed. To address whether changes in the number of cross-bridges and distribution of cross-bridge states could be responsible for differences in sliding speed and E_a between unregulated F-actin and regulated thin filaments at saturating Ca^{2+} , we studied the effects of altered HMM density, and metabolite concentrations which are known to affect the fraction of

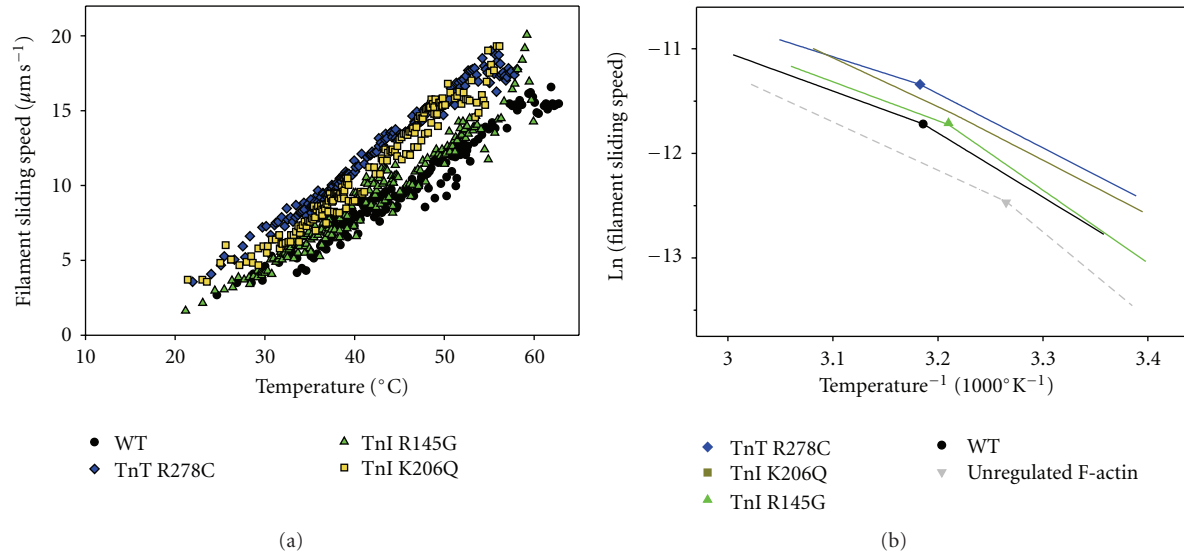


FIGURE 4: Influence of FHC-linked mutations in human cardiac troponin on temperature dependence of thin-filament sliding at pCa 5. Thin filaments were reconstituted with α -Tm and either rhcTn WT (circles, black), rhcTn TnI,R145G (triangles, green), rhcTn TnI,K206Q (squares, yellow), or rhcTn TnT, R278C (diamonds, blue). Data were obtained during the heating phases of multiple heating/cooling cycles, as in Figure 1; note that WT data were replotted from Figure 2(b). (a) Points represent the mean sliding speed for 3–8 filaments during 1 s. Note that speeds with TnI mutant K206Q [32] and TnT mutant R278C were generally elevated over WT. (b) Arrhenius analysis of data from (a). Symbols and colors as in (a); unregulated F-actin from the same series of experiments (Figure 2(b)) was also included in (b) (inverted triangle and dashed lines; light gray). Each dataset was fit by two linear regressions after omitting data above $\sim 60^\circ\text{C}$ (WT), $\sim 54^\circ\text{C}$ (cTnI R145G), $\sim 51.5^\circ\text{C}$ (cTnI K206Q), or $\sim 55^\circ\text{C}$ (cTnT R278C). Regression lines are shown without correction for temperature-dependent changes in solvent viscosity; points correspond to T_i , the intersection of each pair of lines. Filament sliding speeds are expressed in $\mu\text{m s}^{-1}$.

weakly versus strongly bound cross-bridges. Solutions were modified in the following ways, and compared with a control condition that was itself modified in comparison with assays reported in Figures 1–4 (Section 2): decreased [ATP] from 2 mM (Control) to 200 μM , increased [Pi] from $\sim 1 \mu\text{M}$ (Control) to 4 mM, or reduced HMM density (ρ) from 0.25 mg/mL (Control) to 0.075 mg/mL (Figure 5). In these experiments only, motility assays were performed at steady-state temperatures of 27, 32, 37, or 42°C so that we could calculate metabolite concentrations in the presence of CP/CK to buffer ATP/ADP and reduce ADP (Section 2), conditions that did not apply to the nonsteady state temperature assays reported in Figures 1–4.

Sliding speed increased with temperature for each condition tested for both regulated thin filaments at pCa 5 and unregulated F-actin (Figure 5) as expected for the temperature range examined. Sliding speed with respect to the Control condition was reduced significantly for the low ATP condition at the two highest temperatures for unregulated F-actin (Figure 5(a)) and at the three highest temperature points for regulated thin filaments (Figure 5(b)). Sliding speed at high Pi (Figure 5) was higher than in Control conditions at the two lower temperatures for both regulated thin filaments and unregulated F-actin. Decreasing ρ had little effect on unregulated F-actin sliding speed (Figure 5(a)) but decreased regulated thin-filament speed significantly at the three lowest temperatures (27, 32, and 37°C, Figure 5(b)). Addition of Tn·Tm was typically associated with increased speed, but not at low ATP, which

is in good agreement with the results of Homsher et al. [16]. At reduced ρ , the enhancing effect of Tn·Tm was greater at higher temperatures. The fraction of motile filaments at reduced ρ increased over the three lowest temperatures (27, 32, and 37°C) for unregulated F-actin (inset, Figure 5(a)), but over the entire temperature range for regulated thin filaments (inset Figure 5(b)).

4. Discussion

In this study, we utilized microfabricated thermoelectric devices to rapidly and reversibly investigate the influence of temperature on myosin-driven sliding of Ca^{2+} -regulated, muscle thin filaments over a wide temperature range (~ 20 – 60°C). To investigate molecular mechanisms of normal cardiac function and pathophysiology, thin filaments were reconstituted with human cardiac Tn and Tm, or with FHC-related mutants of human cardiac Tn. The major results of this study are as follows.

- At pCa 5, sliding speed of regulated thin filaments increased reversibly with increasing temperature (~ 20 – 54°C) as expected and was faster than unregulated F-actin over that range.
- Reversible dysregulation—loss of Ca^{2+} -regulation—occurred at both pCa 5 and pCa 9 at the upper end of the temperature range examined; this suggests thermal unfolding of the cardiac regulatory proteins and/or their dissociation from actin.

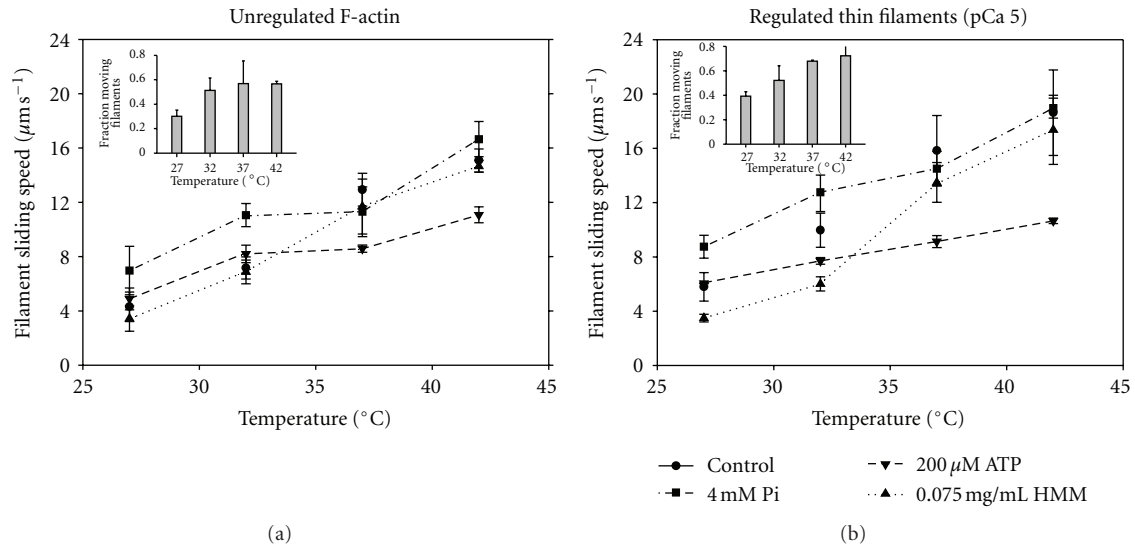


FIGURE 5: Influence of motility conditions on temperature dependence of filament sliding speeds for (a) unregulated F-actin and (b) regulated thin filaments (F-actin plus native cTn and α -Tm) at pCa 5. Points are the mean of means \pm S.D. from 45–75 filaments in each of ≥ 3 individual flow cells and are plotted against steady-state temperature (27–42 $^{\circ}\text{C}$) for four conditions. For this series of experiments only, control conditions (circles, solid lines) were $[\text{Pi}] = \sim 1 \mu\text{M}$ (achieved by removal of contaminating Pi; Section 2); $[\text{ATP}] = 2 \text{ mM}$ (buffered by CP and CK; Section 2), and high ρ achieved by infusing 0.25 mg/mL [HMM] into the flow cell. Conditions were modified to test low ATP (200 μM ATP; inverted triangles, short dashed lines); high Pi (4 mM Pi; squares, long dash dotted lines); or low ρ (0.075 mg/mL HMM; triangles, dash dotted line). Lines were drawn to connect the points. Insets: temperature dependence of fraction of filaments moving under low ρ condition plotted for (a) unregulated F-actin and (b) regulated thin filaments at pCa 5. Note that the fraction of regulated thin filaments, but not unregulated F-actin, increases continuously over this temperature range.

- (c) Arrhenius analysis indicates two temperature regimes with different E_a ; the transition temperature between those regimes was higher for regulated thin filaments than unregulated F-actin, and this is explained by a simple model.
- (d) Factors that alter cross-bridge number and kinetics— $[\text{ATP}]$, $[\text{Pi}]$, and ρ_{HMM} —alter the temperature dependence of sliding speed of both regulated thin filaments and unregulated F-actin in qualitatively similar ways that provide insight into rate limiting factors.
- (e) Three FHC mutants in cTn (cTnI R145G, cTnI K206Q, and cTnT R278C) destabilize regulatory protein structure and/or interactions with F-actin-Tm and may also alter the kinetics of thin filament sliding at pCa 5.

4.1. Functional Assays for Thermal Stability of Regulated Thin Filaments and Ca^{2+} -Regulatory Proteins. A custom thermoelectric controller [5] that was used in this study (Figure 1(a)), and miniaturized versions thereof [6], provide a novel approach to evaluate contractile protein function over a wide range of temperatures and multiple temperature cycles. The multiple datasets collected this way with native and WT regulatory proteins (Figures 1–3) complement and expand the range of information that can be obtained using conventional motility assays [16, 58, 59] and traditional approaches to studying protein structure in solution [60–63]. Our device provides a simpler readout of temperature

than relying on intensity of the fluorescent label [64]. Speed of unregulated F-actin increased monotonically over the temperature range used (Figures 1-2, open symbols), indicating that HMM and actin are not affected detrimentally at temperatures below 60 $^{\circ}\text{C}$; this is consistent with previous functional measurements [5, 64] and structural assays showing that the structure of Ph-stabilized F-actin in solution is thermally stable up to 78 $^{\circ}\text{C}$ [62], while unfolding of subfragment 1 (S1) was reported for temperatures greater than 58 $^{\circ}\text{C}$ in the presence of analogs of ATP or ADP·Pi [63].

Dysregulation of thin filaments at elevated temperatures was observed at both pCa 5 (Figures 1-2) and pCa 9 (Figure 2), suggesting that altered function was likely due to dissociation of Tn·Tm from actin or denaturation of Tn and/or Tm. At pCa 5, the anomalous decline in sliding speed for regulated thin filaments above $\sim 54^{\circ}\text{C}$ suggests a loss of regulation (dysregulation) because as temperature increased, speed decreased toward that of unregulated F-actin (Figure 1(c)). At pCa 9, filament sliding was observed at temperatures above $\sim 43^{\circ}\text{C}$; speed increased with temperature and was generally lower than, but approached that of unregulated F-actin (Figure 2), indicating that cTn stabilizes actin·Tm at pCa 5. Taken together, these results from microthermal heater assays provide functional correlates that are consistent with previous solution studies showing half-maximal dissociation of Tm from Ph-stabilized F-actin·Tm complex (no Tn) at 46–48 $^{\circ}\text{C}$, and unfolding of Tm alone in solution that was resolved into two separate calorimetric domains with maxima of 42 and 51 $^{\circ}\text{C}$ [61, 62]. More generally, our results demonstrate that microthermal

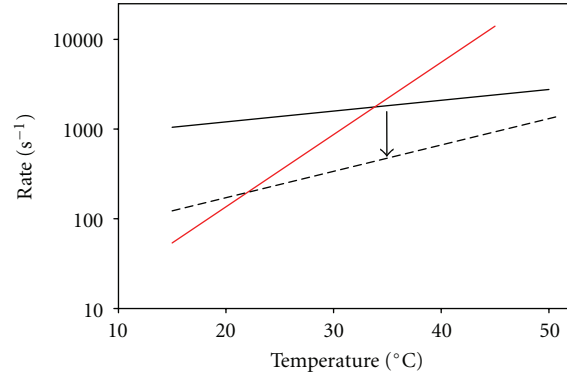


FIGURE 6: Temperature dependence of two apparent rate constants that may limit actin filament sliding speed at pCa 5. Data in Figure 3 ($T < \sim 54^\circ\text{C}$) for sliding speed of regulated thin filaments were fitted to (2). The inverse of each of the exponential rate terms in the denominator of (2) is plotted: for WT regulated thin filaments, one rate exhibits only slight temperature sensitivity (solid black line) while the other is markedly temperature sensitive (red line). The rate-limiting step for filament sliding is the smaller of the two rates, and T_t is the intersection of the two lines. The less temperature sensitive rate is also shown for unregulated F-actin (dashed black line; data from Figure 3). Note that by assuming the temperature-sensitive rate (red line) is similar for both instances, decreasing the less temperature sensitive rate (black arrow, as observed experimentally with unregulated F-actin) decreases T_t .

heater assays can provide unique, molecular level insights into muscle thin-filament function, particularly when the maximum temperature is limited such that the effects of temperature on Ca^{2+} regulation are fully reversible (Figure 2(a)).

4.2. Temperature Dependence of Ca^{2+} -Regulated Thin-Filament Sliding at pCa 5. Comparison of temperature-dependence of regulated thin-filament sliding at pCa 5 with that of unregulated F-actin provides insights into the roles of cardiac troponin and tropomyosin. This is important in light of the observation that not only do Tn-Tm modulate the thin filament side of actomyosin interactions but cTn can also directly accelerate myosin ATPase activity even in the absence of actin and Tm [20]. This direct effect of cTn on myosin kinetics is presumed to at least partially underlie Tn-Tm's enhancement of maximum unloaded sliding speed under a wide variety of conditions (e.g., Figures 1(c), 2(b), 3, 4(b), and 5), although it is also possible that there are differences in the myosin binding interface due to Tm-S1 interactions [65] or regulatory protein-induced structural changes in actin itself [15].

While it is clear that Tn-Tm modulate filament sliding speed primarily by affecting the number of cross-bridges at submaximal Ca^{2+} activation [12, 14, 50], the most straightforward mechanism by which Tn-Tm could directly enhance actomyosin kinetics at saturating Ca^{2+} is through a reduction in the time that cross-bridges spend in the strongly bound state (t_s) under the unloaded conditions of a motility assay, as observed experimentally [33]. The maximum sliding speed (s_m) for regulated thin filaments at saturating Ca^{2+} or for unregulated F-actin is simply related to myosin step size (d_x) and t_s as proposed by Uyeda et al. [51]:

$$s_m = \frac{d_x}{t_s}. \quad (1)$$

To accommodate the observed, biphasic Arrhenius plots (Figures 3 and 4(b)), we assume that $d_x = 0.0055 \mu\text{m}$ [66] for all conditions examined and rewrite (1) to express t_s as the sum of two exponential terms:

$$s_m = \frac{0.0055}{(ae^{-bT} + ce^{-dT})}, \quad (2)$$

which, when fit to the data for regulated thin filaments in Figure 3, yields $s_m = 0.0055 / (0.301e^{-0.1855T} + 0.00145e^{-0.0277T})$ with $R^2 = 0.97$. Separating the two terms and plotting them as rates, we can see that one varies little with temperature (black solid line; Figure 6) and while the other is highly temperature sensitive (red solid line; Figure 6). Assuming that the more highly temperature-dependent term is similar for both regulated thin filaments and unregulated F-actin, regression estimates were obtained for unregulated F-actin sliding in Figure 3, $c = 0.0225$ and $d = 0.0676$ ($R^2 = 0.97$), and the corresponding rate prediction was plotted in Figure 6 (black dashed line).

If the intersections of the red line with the two black lines in Figure 6 are related to discontinuities in the Arrhenius plots (Figures 3 and 4(b)) and thus values of T_t , then the simple analysis of (1), (2) is in accord with observations that the transition from high to low E_a will occur at higher temperature for regulated thin filaments (red and solid black lines) than for unregulated F-actin (red and dashed black lines). In this model, the rate limitation for filament sliding at a given temperature would be the lower of the two rates from the red line and one black line: at low temperatures, the steeper, red value is limiting, while the shallower, black value is limited at elevated temperatures (Figure 6). The temperature dependence of unloaded filament sliding speed has been reported to vary as a function of temperature in some but not all conditions [16, 58, 59]. For unregulated F-actin, Arrhenius plots have been previously reported to be linear within 20–60°C [5] and 7–25°C [16], but nonlinear within 3–42°C with a transition temperature (T_t) of 15.4°C [59],

and 10–35°C with a $T_t \sim 25^\circ\text{C}$ [58, 67]. T_t depends not only on the experimental conditions but also on whether Ca^{2+} -regulatory proteins are present. The Arrhenius plot of fish myofibrillar ATPase at saturating Ca^{2+} exhibited a discontinuity [68], while this was not the case for *in vitro* motility sliding speed and actin-activated MgATPase activity with fish myosin and unregulated F-actin [69]. For regulated thin filaments, Homsher et al. [16] reported a break in the Arrhenius plot around 12.5°C that was not observed for unregulated F-actin within the 7–25°C temperature range. In this study using micromechanical thermal assays, discontinuities in Arrhenius plots for regulated thin filaments (Figures 3 and 4(b)) occurred at a higher temperature than when T_t could be identified for unregulated F-actin (Figure 4(b)). While there is no universal agreement in the limited data available on absolute values for T_t for filament sliding, there does appear to be general agreement that Tn·Tm modulates the temperature dependence of unloaded filament sliding. Our data suggest that this modulation of T_t by human cardiac Tn·Tm occurs around physiological temperature.

The existence of discontinuities in Arrhenius plots suggests that different factors are rate-limiting to filament sliding above and below T_t . What factors could contribute to this difference? Prior experiments with regulated thin filaments at subsaturating levels of Ca^{2+} suggested that the number of cross-bridges is limiting to sliding speed at 30°C [12, 50]. The data in Figure 5 indicate that sliding speed is markedly sensitive to a reduction in the density (ρ) of HMM on the flow cell surface at 27 and 32°C for both unregulated F-actin and especially regulated thin filaments at maximal Ca^{2+} activation. At higher temperatures (37 and 42°C), however, there was little or no effect of the same reduction in ρ on sliding speed for either unregulated F-actin or regulated thin filaments (Figure 5). In addition, the fraction of moving filaments at low ρ increased with temperature for regulated thin filaments at pCa 5 over the entire temperature range (Figure 5(b), inset), while for unregulated F-actin, the fraction started at a lower value and plateaued (Figure 5(a), inset). Taken together, these observations suggest an increase in strong cross-bridges with temperature for both unregulated F-actin and regulated thin filaments, consistent with previous reports using *in vitro* assays and permeabilized muscle fibers [70–72]. Thus, it appears that Tn·Tm can modulate at least one rate-limiting factor, and also T_t , around physiological temperature: once a temperature (T_t) is attained at which the availability of cross-bridges is great enough to guarantee continuous filament sliding, further increase of speed with temperature will only depend on less temperature-sensitive kinetic rates that are associated with transitions between strongly bound cross-bridge states, and will therefore be characterized by low E_a (Figure 6, cross-over from red to black lines).

In addition to the number of cross-bridges, filament sliding speed can be altered by variations in the substrate and products of the ATPase reaction through modulation of actomyosin kinetics. According to the model implicit in (1), changes in metabolite concentration would primarily influence t_s , and therefore s_m , and also the number of

attached cross-bridges. For example, Tn·Tm could affect the kinetics of ATP-induced cross-bridge dissociation that has been suggested to limit filament sliding speed, at least in fast skeletal muscle at low temperature [16, 73]. When [ATP] was reduced to 200 μM —a substrate concentration that is similar to the apparent K_d for sarcomere shortening velocity and filament sliding speed [16, 53, 74, 75]—inhibition of speed was greater for regulated thin filaments at pCa 5 than unregulated F-actin (Figure 5), as reported by Homsher et al. [16]. Inhibition of s_m at low ATP levels is explained by slower ATP-induced detachment of cross-bridges at the end of attached phase the cycle, which increases t_s (1); the fraction of strongly attached cross-bridges would also increase, although the dominant factor in determining s_m in this instance is slower cross-bridge cycling. The relatively greater inhibition of regulated thin-filament sliding was accentuated at higher, more physiological temperatures (Figure 5). The net result was a generally shallow slope of speed versus temperature for both regulated thin filaments and unregulated F-actin (Figure 5) that corresponds to a regime of relatively low E_a . The expectation would then be that reduced [ATP] should shift T_t to a lower temperature (Figure 6) although it was not resolved in this experiment, likely because of the lower limit of temperature examined.

There are some interesting parallels with reduced [ATP] effects, along with significant differences, when the concentration of product Pi was increased from micromolar levels to 4 mM (Table 1), that is, the highest concentration that we could achieve without necessitating an increase in ionic strength. Temperature has previously been shown to modulate the effect of Pi on isometric force in muscle fibers, although there is disagreement about whether Pi is either more [29, 76] or less [77] inhibitory of isometric force as temperature increases. While Pi inhibits isometric force, elevated Pi increases sliding speed for both regulated thin filaments at pCa 5 and unregulated F-actin, although the effect predominates at lower temperatures and is more pronounced for regulated thin-filaments (Figure 5). Maximum velocity of sarcomere shortening [52, 70, 78, 79] and unloaded sliding of unregulated F-actin [80] have previously been reported to increase with elevated Pi. This is generally understood to be the result of reversal of cross-bridge attachment, which decreases t_s as demonstrated at the single molecule level by Baker et al. [81], thus reducing the number of strongly attached cross-bridges and increasing s_m (1). The relatively greater enhancement of sliding speed at lower temperatures results in a generally shallow slope of speed versus temperature for both regulated thin filaments and unregulated F-actin (Figure 5) that corresponds to a regime of relatively low E_a ; in contrast to the result with low ATP, the expectation is that elevated Pi should shift T_t to a higher temperature (Figure 6). Taken together, the data in Figure 5 illustrate that the relative importance of factors which influence cross-bridge cycling kinetics and/or filament sliding speed varies with temperature around the physiological range, and which are rate-limiting also varies as implicated in Figure 6. This suggests that energetic state may impact cardiac function when core body temperature varies,

such as in mild hypothermia or with exercise, in ways that may seem counterintuitive [31].

4.3. Implications for Understanding Cardiovascular Diseases. Figure 4 illustrates that the microthermal heater can be used to study effects of disease-related mutations in human cardiac Ca^{2+} regulatory proteins on function of individual thin filaments. This clearly goes beyond, and will ultimately help explain, prior work that examined physical properties of the mutant proteins in bulk solution, and the Ca^{2+} -dependence of function. cTn mutations may influence not just s_m (TnI K206Q and TnT R278C), but also the temperature dependence of E_a (TnI K206Q and TnT R278C) and possibly T_t (TnI K206Q). The mutations may also influence the temperature at which thin-filament structure is affected to the extent that dysregulation occurs and Ca^{2+} dependent function is altered, whether the disease-related change in function is most relevant in the myofilaments, or perhaps in the nucleus [82]. For all three Tn mutants examined (TnI R145G, TnI K206Q, and TnT R278C) mutations destabilized thin-filament structure and function at lower temperatures than WT; this effect was particularly noticeable for an FHC mutant of human cardiac Tm (E180G) that causes extreme shifts in Ca^{2+} sensitivity [33, 40]. Thus, we anticipate that the thermoelectric heater will be generally useful for characterization of clinically relevant mutants of thin filament protein structural stability through assessment of function at the level of individual thin filaments.

4.4. Conclusion. Results demonstrate the utility of our thermoelectric controller for investigating molecular mechanisms underlying biomolecular motor function, and cardiovascular diseases related to altered biomechanics of cardiac myofilament proteins. This assay provides a novel view of structure-function relationships for cardiac thin filaments.

Acknowledgments

The authors gratefully acknowledge L. A. McFadden for purifying myosin and actin; V. F. Miller for expression and M. Seavy for HPLC purification of tropomyosin; R. Dhanarajan from the Biological Science Molecular Cloning Facility for assistance with mutagenesis; Dr. S. Miller from the Biological Science DNA Sequencing Facility for assistance with DNA sequencing; L. A. Compton for assistance with gel analysis; K. Riddle from the Biological Science Imaging Resource for assistance with MetaMorph; Dr. J. R. Grubich for assistance with preliminary experiments; J. Bhuvorakul and W. Chase for assistance with data analysis; Dr. B. Schoffstall for critical comments. This work was supported by NIH/NHLBI HL63974 (PBC), American Heart Association FL/PR Affiliate 0315097B (NMB), and NSF NIRT Grant ECS-0210332 (PX).

References

- [1] H. Hess, "Toward devices powered by biomolecular motors," *Science*, vol. 312, no. 5775, pp. 860–861, 2006.

- [2] H. Hess and V. Vogel, "Molecular shuttles based on motor proteins: active transport in synthetic environments," *Journal of Biotechnology*, vol. 82, no. 1, pp. 67–85, 2001.
- [3] M. Sundberg, R. Bunk, N. Albet-Torres et al., "Actin filament guidance on a chip: toward high-throughput assays and lab-on-a-chip applications," *Langmuir*, vol. 22, no. 17, pp. 7286–7295, 2006.
- [4] J. A. Jaber, P. B. Chase, and J. B. Schlenoff, "Actomyosin-driven motility on patterned polyelectrolyte mono- and multilayers," *Nano Letters*, vol. 3, no. 11, pp. 1505–1509, 2003.
- [5] G. Mihajlović, N. M. Brunet, J. Trbović, P. Xiong, S. Von Molnár, and P. B. Chase, "All-electrical switching and control mechanism for actomyosin-powered nanoactuators," *Applied Physics Letters*, vol. 85, no. 6, pp. 1060–1062, 2004.
- [6] T. J. Grove, K. A. Puckett, N. M. Brunet et al., "Packaging actomyosin-based biomolecular motor-driven devices for nanoactuator applications," *IEEE Transactions on Advanced Packaging*, vol. 28, no. 4, pp. 556–563, 2005.
- [7] L. Ionov, M. Stamm, and S. Diez, "Reversible switching of microtubule motility using thermoresponsive polymer surfaces," *Nano Letters*, vol. 6, no. 9, pp. 1982–1987, 2006.
- [8] M. S. Parmacek and R. J. Solaro, "Biology of the troponin complex in cardiac myocytes," *Progress in Cardiovascular Diseases*, vol. 47, no. 3, pp. 159–176, 2004.
- [9] J. C. Tardiff, "Thin filament mutations: developing an integrative approach to a complex disorder," *Circulation Research*, vol. 108, no. 6, pp. 765–782, 2011.
- [10] F. Ahmad, J. G. Seidman, and C. E. Seidman, "The genetic basis for cardiac remodeling," *Annual Review of Genomics and Human Genetics*, vol. 6, pp. 185–216, 2005.
- [11] A. M. Gordon, E. Homsher, and M. Regnier, "Regulation of contraction in striated muscle," *Physiological Reviews*, vol. 80, no. 2, pp. 853–924, 2000.
- [12] A. M. Gordon, M. A. LaMadrid, Y. Chen, Z. Luo, and P. B. Chase, "Calcium regulation of skeletal muscle thin filament motility *in vitro*," *Biophysical Journal*, vol. 72, no. 3, pp. 1295–1307, 1997.
- [13] B. Schoffstall, N. M. Brunet, S. Williams et al., " Ca^{2+} sensitivity of regulated cardiac thin filament sliding does not depend on myosin isoform," *Journal of Physiology*, vol. 577, no. 3, pp. 935–944, 2006.
- [14] E. Homsher, B. Kim, A. Bobkova, and L. S. Tobacman, "Calcium regulation of thin filament movement in an *in vitro* motility assay," *Biophysical Journal*, vol. 70, no. 4, pp. 1881–1892, 1996.
- [15] E. Homsher, D. M. Lee, C. Morris, D. Pavlov, and L. S. Tobacman, "Regulation of force and unloaded sliding speed in single thin filaments: effects of regulatory proteins and calcium," *Journal of Physiology*, vol. 524, no. 1, pp. 233–243, 2000.
- [16] E. Homsher, M. Nili, I. Y. Chen, and L. S. Tobacman, "Regulatory proteins alter nucleotide binding to acto-myosin of sliding filaments in motility assays," *Biophysical Journal*, vol. 85, no. 2, pp. 1046–1052, 2003.
- [17] J. A. Gorga, D. E. Fishbaugher, and P. VanBuren, "Activation of the calcium-regulated thin filament by myosin strong binding," *Biophysical Journal*, vol. 85, no. 4, pp. 2484–2491, 2003.
- [18] E. W. Clemmens and M. Regnier, "Skeletal regulatory proteins enhance thin filament sliding speed and force by skeletal HMM," *Journal of Muscle Research and Cell Motility*, vol. 25, no. 7, pp. 515–525, 2004.
- [19] H. Fujita, D. Sasaki, S. Ishiwata, and M. Kawai, "Elementary steps of the cross-bridge cycle in bovine myocardium with and

- without regulatory proteins,” *Biophysical Journal*, vol. 82, no. 2, pp. 915–928, 2002.
- [20] B. Schoffstall, V. A. Labarbera, N. M. Brunet et al., “Interaction between troponin and myosin enhances contractile activity of myosin in cardiac muscle,” *DNA and Cell Biology*, vol. 30, no. 9, pp. 653–659, 2011.
- [21] H. Fujita and M. Kawai, “Temperature effect on isometric tension is mediated by regulatory proteins tropomyosin and troponin in bovine myocardium,” *Journal of Physiology*, vol. 539, no. 1, pp. 267–276, 2002.
- [22] P. P. de Tombe and G. J. M. Stienen, “Impact of temperature on cross-bridge cycling kinetics in rat myocardium,” *Journal of Physiology*, vol. 584, no. 2, pp. 591–600, 2007.
- [23] P. M. L. Janssen, L. B. Stull, and E. Marbán, “Myofilament properties comprise the rate-limiting step for cardiac relaxation at body temperature in the rat,” *American Journal of Physiology*, vol. 282, no. 2, pp. H499–H507, 2002.
- [24] D. A. Martyn, B. B. Adhikari, M. Regnier, J. Gu, S. Xu, and L. C. Yu, “Response of equatorial X-ray reflections and stiffness to altered sarcomere length and myofilament lattice spacing in relaxed skinned cardiac muscle,” *Biophysical Journal*, vol. 86, no. 2, pp. 1002–1011, 2004.
- [25] M. E. Coupland and K. W. Ranatunga, “Force generation induced by rapid temperature jumps in intact mammalian (rat) skeletal muscle fibres,” *Journal of Physiology*, vol. 548, no. 2, pp. 439–449, 2003.
- [26] D. G. Stephenson and D. A. Williams, “Temperature-dependent calcium sensitivity changes in skinned muscle fibres of rat and toad,” *Journal of Physiology*, vol. 360, pp. 1–12, 1985.
- [27] K. W. Ranatunga and S. R. Wylie, “Temperature-dependent transitions in isometric contractions of rat muscle,” *Journal of Physiology*, vol. 339, pp. 87–95, 1983.
- [28] K. W. Ranatunga, “Temperature dependence of mechanical power output in mammalian (rat) skeletal muscle,” *Experimental Physiology*, vol. 83, no. 3, pp. 371–376, 1998.
- [29] E. P. Debold, J. Romatowski, and R. H. Fitts, “The depressive effect of Pi on the force-pCa relationship in skinned single muscle fibers is temperature dependent,” *American Journal of Physiology*, vol. 290, no. 4, pp. C1041–C1050, 2006.
- [30] B. R. MacIntosh, “Role of calcium sensitivity modulation in skeletal muscle performance,” *News in Physiological Sciences*, vol. 18, no. 6, pp. 222–225, 2003.
- [31] J. Weisser, J. Martin, E. Bisping et al., “Influence of mild hypothermia on myocardial contractility and circulatory function,” *Basic Research in Cardiology*, vol. 96, no. 2, pp. 198–205, 2001.
- [32] J. Köhler, Y. Chen, B. Brenner et al., “Familial hypertrophic cardiomyopathy mutations in troponin I (K183Δ, G203S, K206Q) enhance filament sliding,” *Physiological Genomics*, vol. 14, pp. 117–128, 2003.
- [33] F. Wang, N. M. Brunet, J. R. Grubich et al., “Facilitated cross-bridge interactions with thin filaments by familial hypertrophic cardiomyopathy mutations in α -tropomyosin,” *Journal of Biomedicine and Biotechnology*, vol. 2011, Article ID 435271, 12 pages, 2011.
- [34] B. Gafurov, S. Fredricksen, A. Cai, B. Brenner, P. B. Chase, and J. M. Chalovich, “The Δ 14 mutation of human cardiac troponin T enhances ATPase activity and alters the cooperative binding of S1-ADP to regulated actin,” *Biochemistry*, vol. 43, no. 48, pp. 15276–15285, 2004.
- [35] F. Takahashi-Yanaga, S. Morimoto, K. Harada et al., “Functional consequences of the mutations in human cardiac troponin I gene found in familial hypertrophic cardiomyopathy,” *Journal of Molecular and Cellular Cardiology*, vol. 33, no. 12, pp. 2095–2107, 2001.
- [36] R. Lang, A. V. Gomes, J. Zhao, P. R. Housmans, T. Miller, and J. D. Potter, “Functional analysis of a troponin I (R145G) mutation associated with familial hypertrophic cardiomyopathy,” *Journal of Biological Chemistry*, vol. 277, no. 14, pp. 11670–11678, 2002.
- [37] D. Szczesna, R. Zhang, J. Zhao, M. Jones, G. Guzman, and J. D. Potter, “Altered regulation of cardiac muscle contraction by troponin T mutations that cause familial hypertrophic cardiomyopathy,” *Journal of Biological Chemistry*, vol. 275, no. 1, pp. 624–630, 2000.
- [38] F. Yanaga, S. Morimoto, and I. Ohtsuki, “Ca²⁺ sensitization and potentiation of the maximum level of myofibrillar ATPase activity caused by mutations of troponin T found in familial hypertrophic cardiomyopathy,” *Journal of Biological Chemistry*, vol. 274, no. 13, pp. 8806–8812, 1999.
- [39] K. Elliott, H. Watkins, and C. S. Redwood, “Altered regulatory properties of human cardiac troponin I mutants that cause hypertrophic cardiomyopathy,” *Journal of Biological Chemistry*, vol. 275, no. 29, pp. 22069–22074, 2000.
- [40] F. Bai, A. Weis, A. K. Takeda, P. B. Chase, and M. Kawai, “Enhanced active cross-bridges during diastole: molecular pathogenesis of tropomyosin’s HCM mutations,” *Biophysical Journal*, vol. 100, no. 4, pp. 1014–1023, 2011.
- [41] M. C. Mathur, P. B. Chase, and J. M. Chalovich, “Several cardiomyopathy causing mutations on tropomyosin either destabilize the active state of actomyosin or alter the binding properties of tropomyosin,” *Biochemical and Biophysical Research Communications*, vol. 406, no. 1, pp. 74–78, 2011.
- [42] A. Kataoka, C. Hemmer, and P. B. Chase, “Computational simulation of hypertrophic cardiomyopathy mutations in Troponin I: influence of increased myofilament calcium sensitivity on isometric force, ATPase and [Ca²⁺]_i,” *Journal of Biomechanics*, vol. 40, no. 9, pp. 2044–2052, 2007.
- [43] P. B. Chase, Y. Chen, K. L. Kulin, and T. L. Daniel, “Viscosity and solute dependence of F-actin translocation by rabbit skeletal heavy meromyosin,” *American Journal of Physiology*, vol. 278, no. 6, pp. C1088–C1098, 2000.
- [44] S. S. Margossian and S. Lowey, “Preparation of myosin and its subfragments from rabbit skeletal muscle,” *Methods in Enzymology*, vol. 85, no. C, pp. 55–71, 1982.
- [45] J. D. Pardee and J. Aspidich, “Purification of muscle actin,” *Methods in Enzymology*, vol. 85, no. C, pp. 164–181, 1982.
- [46] R. W. Heald and S. E. Hitchcock-DeGregori, “The structure of the amino terminus of tropomyosin is critical for binding to actin in the absence and presence of troponin,” *Journal of Biological Chemistry*, vol. 263, no. 11, pp. 5254–5259, 1988.
- [47] P. B. Monteiro, R. C. Lataro, J. A. Ferro, and F. D. C. Reinach, “Functional α -tropomyosin produced in *Escherichia coli*. A dipeptide extension can substitute the amino-terminal acetyl group,” *Journal of Biological Chemistry*, vol. 269, no. 14, pp. 10461–10466, 1994.
- [48] H. Schagger and G. Von Jagow, “Tricine-sodium dodecyl sulfate-polyacrylamide gel electrophoresis for the separation of proteins in the range from 1 to 100 kDa,” *Analytical Biochemistry*, vol. 166, no. 2, pp. 368–379, 1987.
- [49] S. J. Kron, Y. Y. Toyoshima, T. Q. P. Uyeda, and J. A. Spudich, “Assays for actin sliding movement over myosin-coated surfaces,” *Methods in Enzymology*, vol. 196, pp. 399–416, 1991.

- [50] B. Liang, Y. Chen, C. K. Wang et al., "Ca²⁺ regulation of rabbit skeletal muscle thin filament sliding: role of cross-bridge number," *Biophysical Journal*, vol. 85, no. 3, pp. 1775–1786, 2003.
- [51] T. Q. P. Uyeda, S. J. Kron, and J. A. Spudich, "Myosin step size estimation from slow sliding movement of actin over low densities of heavy meromyosin," *Journal of Molecular Biology*, vol. 214, no. 3, pp. 699–710, 1990.
- [52] E. Pate and R. Cooke, "Addition of phosphate to active muscle fibers probes actomyosin states within the powerstroke," *Pflügers Archiv*, vol. 414, no. 1, pp. 73–81, 1989.
- [53] P. B. Chase and M. J. Kushmerick, "Effect of physiological ADP concentrations on contraction of single skinned fibers from rabbit fast and slow muscles," *American Journal of Physiology*, vol. 268, no. 2, pp. C480–C489, 1995.
- [54] R. Silverstein, J. Voet, D. Reed, and R. H. Abeles, "Purification and mechanism of action of sucrose phosphorylase," *Journal of Biological Chemistry*, vol. 242, no. 6, pp. 1338–1346, 1967.
- [55] R. C. Weast, *CRC Handbook of Chemistry and Physics*, CRC Press, Boca Raton, Fla, 1982, 63rd edition, 1982.
- [56] P. B. Chase, T. M. Denking, and M. J. Kushmerick, "Effect of viscosity on mechanics of single, skinned fibers from rabbit psoas muscle," *Biophysical Journal*, vol. 74, no. 3, pp. 1428–1438, 1998.
- [57] A. V. Gomes and J. D. Potter, "Molecular and cellular aspects of troponin cardiomyopathies," *Annals of the New York Academy of Sciences*, vol. 1015, pp. 214–224, 2004.
- [58] R. Rossi, M. Maffei, R. Bottinelli, and M. Canepari, "Temperature dependence of speed of actin filaments propelled by slow and fast skeletal myosin isoforms," *Journal of Applied Physiology*, vol. 99, no. 6, pp. 2239–2245, 2005.
- [59] M. Anson, "Temperature dependence and arrhenius activation energy of F-actin velocity generated *in vitro* by skeletal myosin," *Journal of Molecular Biology*, vol. 224, no. 4, pp. 1029–1038, 1992.
- [60] N. Golitsina, Y. An, N. J. Greenfield et al., "Effects of two familial hypertrophic cardiomyopathy-causing mutations on α -tropomyosin structure and function," *Biochemistry*, vol. 38, no. 12, p. 3850, 1999.
- [61] E. V. Kremneva, O. P. Nikolaeva, N. B. Gusev, and D. I. Levitsky, "Effects of troponin on thermal unfolding of actin-bound tropomyosin," *Biochemistry*, vol. 68, no. 7, pp. 802–809, 2003.
- [62] E. Kremneva, S. Boussouf, O. Nikolaeva, R. Maytum, M. A. Geeves, and D. I. Levitsky, "Effects of two familial hypertrophic cardiomyopathy mutations in α -tropomyosin, Asp175Asn and Glut180Gly, on the thermal unfolding of actin-bound tropomyosin," *Biophysical Journal*, vol. 87, no. 6, pp. 3922–3933, 2004.
- [63] J. W. Shriver and U. Kamath, "Differential scanning calorimetry of the unfolding of myosin subfragment 1, subfragment 2, and heavy meromyosin," *Biochemistry*, vol. 29, no. 10, pp. 2556–2564, 1990.
- [64] H. Kato, T. Nishizaka, T. Iga, K. Kinoshita, and S. Ishiwata, "Imaging of thermal activation of actomyosin motors," *Proceedings of the National Academy of Sciences of the United States of America*, vol. 96, no. 17, pp. 9602–9606, 1999.
- [65] P. Vibert, R. Craig, and W. Lehman, "Steric-model for activation of muscle thin filaments," *Journal of Molecular Biology*, vol. 266, no. 1, pp. 8–14, 1997.
- [66] C. Veigel, M. L. Bartoo, D. C. S. White, J. C. Sparrow, and J. E. Molloy, "The stiffness of rabbit skeletal actomyosin cross-bridges determined with an optical tweezers transducer," *Biophysical Journal*, vol. 75, no. 3, pp. 1424–1438, 1998.
- [67] P. Höök and L. Larsson, "Actomyosin interactions in a novel single muscle fiber *in vitro* motility assay," *Journal of Muscle Research and Cell Motility*, vol. 21, no. 4, pp. 357–365, 2000.
- [68] T. S. Moerland and B. D. Sidell, "Contractile responses to temperature in the locomotory musculature of striped bass *Morone saxatilis*," *Journal of Experimental Zoology*, vol. 240, no. 1, pp. 25–33, 1986.
- [69] T. J. Grove, L. A. Mcfadden, P. B. Chase, and T. S. Moerland, "Effects of temperature, ionic strength and pH on the function of skeletal muscle myosin from a eurythermal fish, *Fundulus heteroclitus*," *Journal of Muscle Research and Cell Motility*, vol. 26, no. 4-5, pp. 191–197, 2005.
- [70] M. Kawai, K. Kawaguchi, M. Saito, and S. Ishiwata, "Temperature change does not affect force between single actin filaments and HMM from rabbit muscles," *Biophysical Journal*, vol. 78, no. 6, pp. 3112–3119, 2000.
- [71] C. Karatzaferi, M. K. Chinn, and R. Cooke, "The force exerted by a muscle cross-bridge depends directly on the strength of the actomyosin bond," *Biophysical Journal*, vol. 87, no. 4, pp. 2532–2544, 2004.
- [72] Y. Zhao and M. Kawai, "Kinetic and thermodynamic studies of the cross-bridge cycle in rabbit psoas muscle fibers," *Biophysical Journal*, vol. 67, no. 4, pp. 1655–1668, 1994.
- [73] M. Nyitrai, R. Rossi, N. Adamek, M. A. Pellegrino, R. Bottinelli, and M. A. Geeves, "What limits the velocity of fast-skeletal muscle contraction in mammals?" *Journal of Molecular Biology*, vol. 355, no. 3, pp. 432–442, 2006.
- [74] R. Cooke and W. Bialek, "Contraction of glycerinated muscle fibers as a function of the ATP concentration," *Biophysical Journal*, vol. 28, no. 2, pp. 241–258, 1979.
- [75] E. Pate, M. Lin, K. Franks-Skiba, and R. Cooke, "Contraction of glycerinated rabbit slow-twitch muscle fibers as a function of MgATP concentration," *American Journal of Physiology*, vol. 262, no. 4, pp. C1039–C1046, 1992.
- [76] E. P. Debold, H. Dave, and R. H. Fitts, "Fiber type and temperature dependence of inorganic phosphate: implications for fatigue," *American Journal of Physiology*, vol. 287, no. 3, pp. C673–C681, 2004.
- [77] M. E. Coupland, E. Puchert, and K. W. Ranatunga, "Temperature dependence of active tension in mammalian (rabbit psoas) muscle fibres: effect of inorganic phosphate," *Journal of Physiology*, vol. 536, no. 3, pp. 879–891, 2001.
- [78] P. B. Chase and M. J. Kushmerick, "Effects of pH on contraction of rabbit fast and slow skeletal muscle fibers," *Biophysical Journal*, vol. 53, no. 6, pp. 935–946, 1988.
- [79] C. Karatzaferi, K. Franks-Skiba, and R. Cooke, "Inhibition of shortening velocity of skinned skeletal muscle fibers in conditions that mimic fatigue," *American Journal of Physiology*, vol. 294, no. 3, pp. R948–R955, 2008.
- [80] E. Homsher, F. Wang, and J. R. Sellers, "Factors affecting movement of F-actin filaments propelled by skeletal muscle heavy meromyosin," *American Journal of Physiology*, vol. 262, no. 3, pp. C714–C723, 1992.
- [81] J. E. Baker, C. Brosseau, P. B. Joel, and D. M. Warshaw, "The biochemical kinetics underlying actin movement generated by one and many skeletal muscle myosin molecules," *Biophysical Journal*, vol. 82, no. 4, pp. 2134–2147, 2002.
- [82] F. Z. Asumda and P. B. Chase, "Nuclear cardiac troponin and tropomyosin are expressed early in cardiac differentiation of rat mesenchymal stem cells," *Differentiation*, vol. 83, no. 2, pp. 106–115.